Ultrasound in Med. & Biol., Vol. 26, No. 9, pp. 1445–1453, 2000

0301-5629/00/$–see front matter

PII: S0301-5629(00)00289-1

● *Original Contribution*

ECHOCARDIOGRAPHIC TEXTURE ANALYSIS USING THE WAVELET TRANSFORM: DIFFERENTIATION OF EARLY HEART MUSCLE DISEASE

EDMUND K. KERUT,* MICHAEL B. GIVEN,* ELIZABETH MCILWAIN,* GAYLE ALLEN,* C. ESPINOZA† and THOMAS D. GILES*

*Cardiovascular Research Laboratory, Division of Cardiology and †Department of Pathology, Louisiana State University Health Sciences Center, New Orleans, LA, USA

(*Received* 18 *February* 2000; *in final form* 6 *July* 2000)

Abstract—Echocardiographic quantitation of myocardial texture for diagnosis of early cardiomyopathy (CMP) remains problematic. Conventional statistical methods are limited, contributed by a small image region-of-interest (ROI) and difficulty in discrimination from noise. This study was performed to evaluate the 2-D Haar wavelet decomposition method as a tool to identify textural changes in a rat model of early CMP, focusing on changes that occur before development of M-mode structural abnormalities. Early diabetic CMP, ethanol CMP and diabetic-ethanol CMP rat models were evaluated. Echocardiography was performed on two groups of rats. Group I (5 week cohort, $n = 4$ per subgroup) included controls, rats on 12% ethanol, a diabetic subgroup, and diabetic rats on 4% ethanol. Group II (10 week cohort, $n = 5$ per subgroup) included the same categories as group I with an additional subgroup taking 4% ethanol was also studied. M-mode left ventricular measurements were comparable in all subgroups of group I. However, diabetic rats in group II had an increased left ventricular dimension (LVD) compared to all others and an increased septal dimension (IVSD) and posterior wall dimension (PWD) were noted in the 4% and 12% ethanol groups. End-diastolic digital images of all rats in the parasternal short axis view, at the papillary muscle level, were downloaded to a computer. A 16 × 16 (ROI) was selected from the anterior interventricular septum. Although standard statistical methods could not differentiate any of the groups, calculation of textural energy and normalized textural energy with the 2-D Haar wavelet decomposition method found at 5 weeks increased normalized texture energy in diabetics compared to all others. At 10 weeks increased texture energy was noted in diabetics. Diabetic-ethanol rats at both 5 and 10 weeks revealed a blunted textural energy compared to diabetic rats. In a rat model of diabetic cardiomyopathy, the 2-D wavelet decomposition method identified textural energy changes before development of echocardiographic structural changes. Ethanol-associated blunting of textural changes in diabetic rats was also noted. This method for quantitation of ventricular texture may be relevant for diagnosis of early cardiomyopathy. © 2001 World Federation for Ultrasound in Medicine & Biology.

Key Words: **Ultrasound, Echocardiography, Texture, Texture energy, Myocardial texture, Wavelet, Wavelet decomposition, Haar, Diabetic cardiomyopathy, Ethanol cardiomyopathy.**

INTRODUCTION

Detection and quantitative assessment of diseased tissue is a challenge for noninvasive imaging techniques. Direct histologic or biochemical means are limited by their requirement for interventional procedures. To better characterize the onset and progression of cardiomyopathy, a noninvasive imaging technique for distinguishing normal from abnormal tissue would be of particular importance. Texture analysis of myocardium is an approach to tissue characterization based on the spatial distribution of ultrasound (US) amplitude signals within a region-of-interest ROI. The characterization of myocardial tissue itself by US was first attempted in 1957 when excised human hearts were used to distinguish infarcted from healthy myocardium (Wild et al. 1957).

Echocardiographic methods to characterize myocardium have included quantitative estimates of frequency-dependent myocardial attenuation and backscatter (Miller et al. 1985), and have subsequently been used to distinguish normal from abnormal myocardium (Haskell

Address correspondence to: Edmund K. Kerut, M.D., 1111 Medical Center Blvd., Suite N613, Marrero, LA 70072 USA. E-mail: ekerut@pol.net

et al. 1990; Sagar et al. 1987, 1990; Wickline et al. 1986).

One definition of image texture is "an attribute representing the spatial arrangement of the gray levels of the pixels in a region" (IEEE 1990). Although myocardial speckle is transducer- and instrument-dependent, tissue pathology that changes microscopic anatomical structure changes myocardial texture (speckle), and echocardiographic texture does contain tissue structure-related information (Smith and Wagner 1994; Wagner et al. 1983). Attempting to numerically quantitate texture, however, has been generally problematic with respect to the myocardium.

Bhandari and Nanda (1983) described a qualitative approach to texture patterns of myocardium based on visual inspection of videotaped 2-D echocardiograms from patients with a variety of disorders. They proposed a classification system based on the textural patterns visualized as: type I (uniform, low intensity, fine speckle: normal), type IIA (multiple, discrete, 3 to 5 mm, bright echoes in all walls), type IIB (one or more, but not all, walls with type IIA pattern) and type IIC (uniform very bright echoes in one wall or region). This approach remains subjective, and lacks specificity.

Quantitation of texture using statistical techniques has been performed to identify various cardiomyopathic abnormalities, including myocardial contusion (Skorton et al. 1983a), amyloid infiltration (Pinamonti et al. 1989), hypertrophic cardiomyopathy (Chandrasekaran et al. 1989), coronary ischemia (Picano et al. 1993), myocardial nonviability (Marini et al. 1996), transplant rejection (Stempfle et al. 1993) and myocarditis (Ferdeghini et al. 1991). These published studies used first- or second-order grey-level histogram statistics for evaluation (usually 8 bits information), including mean grey level, standard deviation of the mean, skewness (deviation of the pixel distribution from a symmetrical shape) and the kurtosis (steepness of the pixel distribution).

The above-described statistical methods used for quantitation of myocardial texture have limited capability. Data content for analysis was diminished in most of these studies because they were performed with digitized video signals for analysis. In addition, the ROI was relatively small ($\approx 16 \times 16$ pixel matrix) to avoid specular reflections (endocardial and epicardial borders). This small ROI limits the capability of statistical methodologies.

A relatively new mathematical tool called wavelet analysis has been introduced within the recent past as a way to look at a signal at different resolutions (Aldroubi 1996; Daubechies 1992; Teolis 1998; Unser 1996). Briefly, a wavelet is a waveform of limited duration that has an average value of zero. Wavelet analysis involves the breaking up of a signal into shifted and scaled versions of the original "mother" wavelet. Mallat (1989a, 1989b) developed the dyadic wavelet method of multiresolution analysis, particularly useful for image processing. In effect, this method decomposes a signal into a set of approximation coefficients (low-frequency components) and the remainder as the detail coefficients (high-frequency components). The approximation coefficients can be successively decomposed into multilevel approximation coefficients and their corresponding detail coefficients. When one is analyzing a 2-D signal, such as an image, at each level of decomposition there are three sets of generated detail coefficients: horizontal (vertical edge), vertical (horizontal edge), and diagonal.

One-dimensional wavelets are used in analysis of various time-domain signals including evoked potentials (Bertrand et al. 1994), heart rate variability analysis (Gamero et al. 1996) and ventricular late potentials (Batista and English 1996; Meste et al. 1994). Two-dimensional wavelets have been used for image compression. The approximation coefficients are utilized, and the detail coefficients are generally discarded (Chui 1997; Press et al. 1992; Wickerhauser 1994). These detail coefficients contain noise and artefact, but also contain textural information (Prasad and Lyengar 1997). The generated detail coefficients have been used for quantitation of texture of various surfaces (Prasad and Lyengar 1997), texture analysis in satellite remote sensing (Mecocci et al. 1995) and US texture analysis for characterization of fat content and marbling in beef cattle muscle (Kim et al. 1998).

Recently, investigators used the Haar wavelet transform, with an image extension method and wavelet decomposition, to calculate texture energy and differentiate viable from nonviable myocardium (Mojsilovic et al. 1997; Neskovic et al. 1998). We used the wavelet decomposition method with the 2-D Haar wavelet transform to see if calculated textural energy would differentiate echocardiographic myocardial tissue texture between euglycemic and diabetic rats. We also examined the influence of ethanol on the development of textural changes in these animals. We studied the interaction of diabetes mellitus and ethanol because we have previously demonstrated a positive benefit of ethanol on cell-signaling abnormalities produced by diabetes mellitus (unpublished observations).

Unlike previous studies, we avoided use of the generated video signal, which requires analog-to-digital conversion. We utilized digital images (8-bit RGB signal) immediately after digital scan conversion, without image smoothing or logarithmic compression.

METHODS

Rodent models of cardiomyopathy

Two groups of laboratory rats were used to perform two separate experiments. Male Sprague-Dawley SPF rats (Charles River Laboratories, Wilmington, MA) weighing between 175 to 200 G were used for each study. Rats were housed two per cage in a controlled-temperature (20 to 22°C) room where they were exposed to a 12-h light/dark cycle. Both groups of animals received food and either water or ethanol *ad lib*. Body weights were recorded on a weekly basis and fluid consumption was monitored in all groups for the duration of the study. The study was approved by the Louisiana State University Medical Center Institutional Animal Care and Use Committee.

Group I

A total of 16 rats were randomly assigned to four groups ($n = 4$ per subgroup): control (C), 12% ethanol (E12), diabetic (D), and diabetic maintained on 4% ethanol (DE4). Ethanol solutions were prepared on a v/v basis and were the sole source of fluid for E12 and DE4 groups; C and D groups received water. Rats in the diabetic group were injected with streptozotocin (45 mg/kg) prepared in a 0.02 M sodium citrate solution (pH 4.5) *via* a tail vein to induce diabetes mellitus. Rats assigned to all other groups were injected with a similar volume of sodium citrate solution. Glycosylated hemoglobin (total) was measured in tail-vein blood in all rats within 2 days of echocardiographic examination using a commercially available kit (Sigma Chemical Co., St. Louis, MO). All diabetic rats exhibited the clinical signs of polydipsia, polyuria and polyphagia. A 4% ethanol solution was used in the diabetes plus ethanol group because diabetic animals consumed approximately 3 times the volume of fluid per day compared with nondiabetic groups. Animals were studied 5 weeks poststreptozotocin injection (4 weeks ethanol ingestion).

Group II

A second experiment was similar in design, but examined rats at 10 weeks after streptozotocin injection in the diabetic animals (9 weeks ethanol ingestion). Subgroups and randomization strategy were similar to the 5-week experiment, but an additional subgroup (fifth subgroup) was added to examine nondiabetic rats given 4% (v/v) ethanol in their water supply (designated DE4). A total of 25 rats were used in this experiment, with 5 animals in each group.

Echocardiography

All animals were anesthetized with a solution of ketamine-xylazine (50 mg/kg ketamine, 4 mg/kg xylazine, IP) and the thoracic and upper abdominal areas shaved before echocardiography. The rats were positioned on a table for M-mode and 2-D echocardiograms. Studies were performed with a Toshiba Model 380 Echocardiography instrument (Toshiba America Medical Systems, Tustin, CA) using a 10-MHz phased-array transducer calibrated with phantoms before use. The transducer uses multiple transmit foci, and dynamic focusing by an internal circuit on receive. The image depth was set as 4 cm and focus of 1 cm for the entire study. Lateral resolution less than 0.20 mm and an axial resolution of 0.2 mm within the ROI is achieved at the imaging depths used (Personal communication, K. Ishiyama, Toshiba America Medical Systems, Inc., Tustin, CA).

M-mode recordings, using 2-D parasternal short axis guidance, were obtained at the level of the papillary muscles for measures of the end-diastolic interventricular septal dimension (IVSD), left ventricular end-diastolic dimension (LVD) and end-diastolic posterior wall dimension (PWD), following American Society of Echocardiography guidelines for M-mode measurements (Sahn et al. 1978). End-diastole was defined as the largest 2-D cross-sectional area.

For texture analysis, digital images were obtained immediately after digital scan conversion. Digital smoothing or logarithmic compression was not performed. Gain settings were kept constant throughout the entire study. Two-dimensional echocardiographic images in the parasternal short axis, at the level of the papillary muscles, were digitally recorded in end-diastole. The end-diastolic image was downloaded as an RGB signal in DEFF format to a laptop computer. The image was converted to a grey-scale image (8 bit) and stored as a TIFF file. From this image, a 16×16 pixel ROI was selected in the anterior IVS. Care was taken to only select myocardium within the ROI, excluding endocardial and epicardial borders; thus, avoiding specular reflections.

Analysis of texture was first performed using traditional statistical methods. These included measurement of ROI mean intensity, standard deviation of the mean, skewness, kurtosis and relative smoothness *RS*, as $RS = 1–1/(1 + V^2)$, and V is the variance of ROI pixel intensity (Gonzales and Woods 1992).

Computer algorithms developed in our laboratory for applying the 2-D wavelet decomposition method were then used to examine the defined ROI. The original image ROI was decomposed into approximation coefficients and the residual horizontal (H1), vertical (V1), and diagonal (D1) detail coefficients (Fig. 1).

Texture content information was obtained by calculating the energy content of the first level detail coefficients from the image ROI (Prasad and Lyengar 1997; Van de Wouwer et al. 1999; Chang and Kuo 1993). H1,

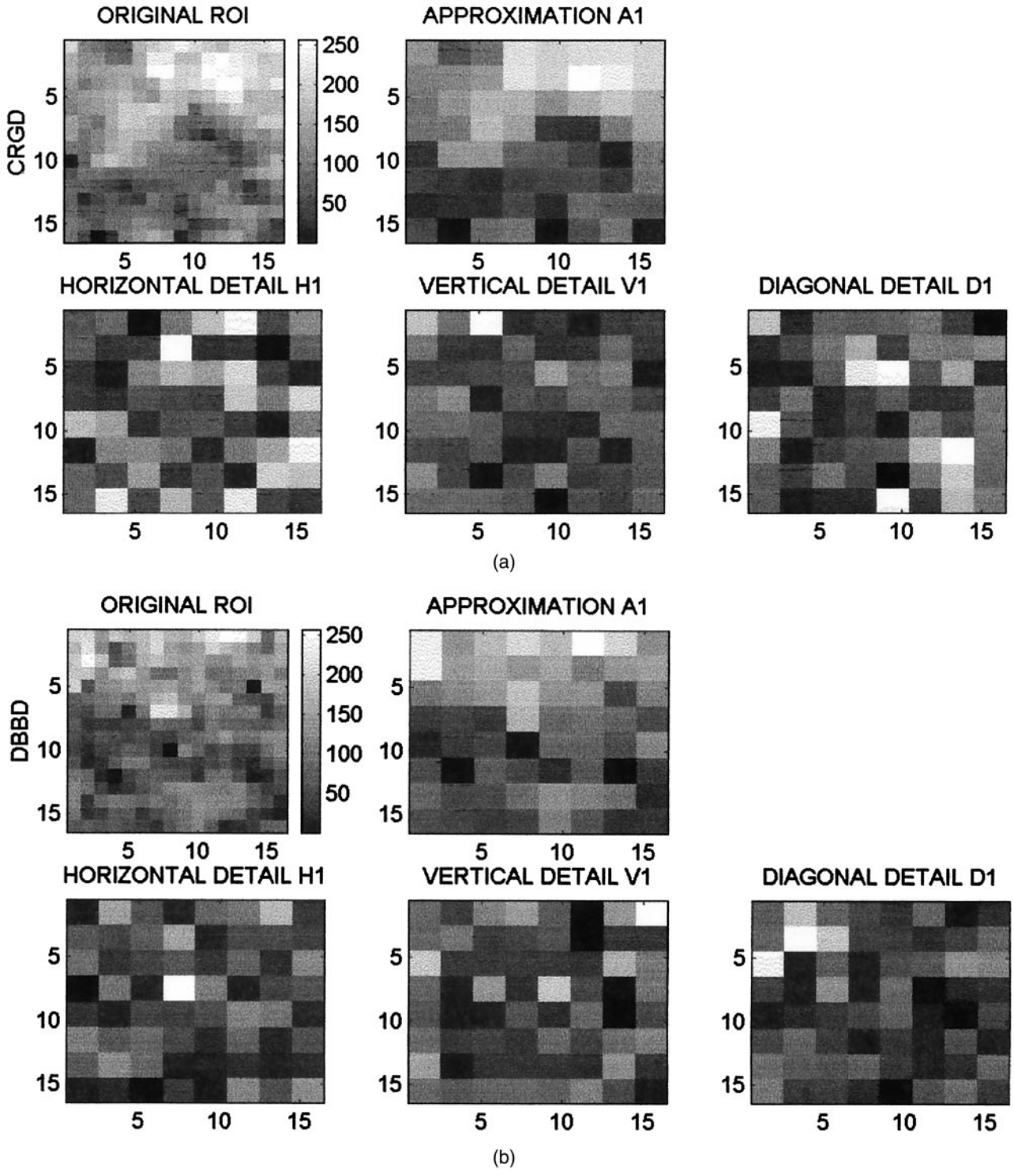

Fig. 1. Example from (a) a control and (b) diabetic rat after 5 weeks of induced diabetes. An end-diastolic parasternal short axis preprocessed frame at the level of the papillary muscles was saved and a 16 × 16 ROI chosen within the anterior interventricular septum. This ROI was converted to grey-scale (original ROI) in (a) and (b). Two-dimensional Haar wavelet decomposition was performed, and approximation coefficients and residual detail coefficients obtained. Approximation (A1) in (a) and (b) shows the reconstructed approximation images from the approximation coefficients and horizontal (H1), vertical (V1) and diagonal (D1) reconstructed detail images from the corresponding detail coefficients.

V1, and D1 were each evaluated for energy content *E*, as $E = (1/N) * \Sigma I^2$ where *N* is the number of pixels within the ROI, and *I* is the pixel intensity values (Walker 1999).

Horizontal and vertical, and also horizontal, vertical and diagonal detail coefficients were summed to yield total energy within detail coefficients. Calculated energy values were also normalized to the energy content of the original ROI image energy.

Myocardial histology

In experiment 2 (10-week), cardiac and renal tissues were harvested, rinsed in ice-cold physiologic saline, and then placed in 10% (v/v) formaldehyde solution in aqueous phosphate buffer (pH 7.4) (Mallinckrodt Inc., St. Louis, MO). Pancreatic tissue was harvested and fixed in buffered zinc-formaldehyde. Microscopic analyses were performed on H & E stained tissue slices.

Statistical methods

A one-way analysis of variance was used to test for differences among the experimental groups. The Fisher's Protected LCD *post hoc* test was used to identify groups that were statistically different from each other. Statistical significance was accepted if $p \leq 0.05$. Simple linear regression was used to determine the relationship between the variance of the image ROI pixel intensity and detail coefficients obtained from calculation of image energy, log energy, and Shannon's entropy (Coifman and Wickerhauser 1992) following wavelet decomposition. All data are reported as mean ± SEM.

RESULTS

Induction of diabetes

In group I, glycosylated hemoglobin (total) levels in normoglycemic groups were not statistically different and had combined means of 5.6 ± 0.7%. Diabetic subgroups had similar glycosylated hemoglobin levels as well, with a combined mean of 10.8 ± 1.1%. These levels of glycosylated hemoglobin were significantly greater in diabetic compared to nondiabetic animals ($p \leq 0.001$). Body weights at the time of echocardiographic examination were 315 ± 15, 301 ± 11, 298 ± 16, 292 ± 22 G for C, E12, D and DE4, respectively ($p \geq 0.05$). In group II, total glycosylated hemoglobin levels within nondiabetic (C, E4, E12) and diabetic subgroups (D, DE4) were, again, not different statistically, with combined means of 6.1 ± 0.3% and 12.5 ± 1.3%, respectively. Again, diabetic animals had significantly greater glycosylation levels compared with normoglycemic animals ($p \leq 0.001$). Group differences in body weights were observed at 10 weeks with both the D (315 ± 24 G) and DE4 (295 ± 16 G) groups weighing significantly less than the normoglycemic groups (623 ± 30, 598 ± 29 and 581 ± 25 G for C, E4 and E12, respectively; $p \leq 0.001$). Although diabetic animals weighed less than their nondiabetic counterparts, they continued to gain weight during the experiment, as can be seen when compared to initial start weights of 175 to 200 G.

Ethanol

The 4% solution of alcohol in diabetic rats was equivalent to 12% alcohol in euglycemic rats, because diabetic animals drank approximately 3 times the amount consumed by euglycemic rats (118 ± 5 mL/day vs. 32 ± 3 mL/day, respectively). The amount of fluid consumed by diabetic rats maintained on water and diabetic rats on 4% alcohol was not statistically different.

Histology

Tissues from 10-week treated rats were analyzed using H & E staining. Both diabetic groups (D, DE4) showed marked loss of pancreatic islet β cells (a single cell was observed in 1 D animal) and the euglycemic control and ethanol groups had the normal complement of β cells. In addition, clear cells, indicative of glycogen deposition, were observed in the kidney in 80% of D and 60% of DE4 rats; none were observed in rats from any other group.

It was noted that the myocardial IVS of all animals in the E4 and E12 groups had marked lymphocytic infiltrates on histologic examination. The degree of infiltration was evaluated qualitatively as none, few (1 to 4 cells per field), or marked infiltration. Only 2 control animals, and 1 diabetic (D) animal, had lymphocytic infiltrates (graded as few). The remaining animals in these groups did not show infiltrates, nor did any animal of the DE group.

Echocardiographic analysis—M-mode measurements

Analysis of M-mode echocardiographic data (IVSD, PWD, or LVD) revealed no statistically significant differences between groups in the 5-week experiment. However, significant differences were found with several measured M-mode parameters in the 10-week experiment (Table 1). Ethanol-treated nondiabetic animals showed increases in IVSD and PWD at 10 weeks, with the effects being most pronounced in animals on 12% ethanol. LVD was increased in diabetic animals on water, but PWD tended to be reduced in these animals and in diabetic rats maintained on 4% ethanol.

Echocardiographic texture analysis

Of the 25 rats in the 10-week experiment, 1 rat (D group) could not be included in the texture analysis because of an inability to obtain a 16 × 16 pixel ROI within the anterior IVS that would exclude specular

Table 1. Myocardial M-mode measurements

	IVSD (cm)	PWD (cm)	LVD (cm)
Experiment 1 (5 weeks)			
Control	0.120 ± 0.006	0.132 ± 0.007	0.455 ± 0.035
Ethanol (12%)	0.130 ± 0.007	0.150 ± 0.003	0.540 ± 0.027
Diabetic	0.118 ± 0.009	0.142 ± 0.010	0.507 ± 0.042
Diabetic + 4% ethanol	0.120 ± 0.004	0.143 ± 0.005	0.455 ± 0.027
ANOVA	$p \leq 0.564$	$p \leq 0.202$	$p \leq 0.444$
Experiment 2 (10 weeks)			
Control	0.117 ± 0.008	0.140 ± 0.006	0.614 ± 0.028
Ethanol (4%)	0.126 ± 0.01*	0.155 ± 0.005‡	0.583 ± 0.033
Ethanol (12%)	0.151 ± 0.004†	0.159 ± 0.002‡	0.593 ± 0.018
Diabetic	0.111 ± 0.004	0.128 ± 0.002	0.713 ± 0.036†
Diabetic + ethanol (4%)	0.105 ± 0.005	0.125 ± 0.004§	0.618 ± 0.032
ANOVA	$p \leq 0.002$	$p \leq 0.001$	$p \leq 0.045$

* $p \leq 0.05$ vs. DE4; † $p \leq 0.05$ vs. all other groups in the appropriate experiment; ‡ $p \leq 0.05$ vs. C, D, DE4; § $p \leq 0.05$ vs. C.

reflections. Therefore, only 4 animals were used for texture analysis in this diabetic group.

Quantitation of ROI texture by standard statistical methods (mean intensity, variance, standard deviation of the mean, skewness or kurtosis) did not identify any intergroup differences at either 5 or 10 weeks. In addition, calculation of the relative smoothness of the ROI was also unable to discriminate between groups at either time period. However, image decomposition using the 2-D Haar wavelet method for calculation of detail coefficient energy did identify diabetic animals as having increased textural energy at 10 weeks. The horizontal detail coefficient (H1) approached significance in ability to differentiate experimental groups ($p \cong 0.07$); vertical (V1), diagonal (D1), H1 + V1 and H1+V1+D1 detail coefficients were all able to statistically discriminate groups (Table 2). Normalization of the detail coefficients to total energy of the original digital image resulted in the identification of increased textural energy in the diabetic animals at 5 weeks. This finding is consistent with the 10-week nonnormalized data. In addition, again consistent with the 10-week data, ethanol-treated diabetic rats tended to show reduced textural energy values compared with untreated diabetic rats (Table 3).

DISCUSSION

Echocardiographic texture analysis using digital images that had not been processed with smoothing or logarithmic compression, and the 2-D Haar wavelet transform decomposition method, discriminated between rodent models of cardiomyopathy. These textural changes were present before development of structural changes recorded by M-mode echocardiography. Subsequent development of M-mode changes at 10 weeks were similar to those observed by our group (Giles et al.

Table 2. Image texture energy calculation

	Total image energy	Approximation coefficients (A1)	Horizontal detail (H1)	Vertical detail (V1)	Diagonal detail (D1)	H1 + V1	H1 + V1 + D1
Experiment 1 (5 weeks)							
Control	3288 ± 620	12830 ± 2438	170 ± 30	134 ± 19	31 ± 3	293 ± 46	324 ± 48
Ethanol (12%)	4846 ± 66*	18870 ± 2582	278 ± 46	189 ± 34	50 ± 6	467 ± 77	517 ± 83
Diabetic	2401 ± 631	9206 ± 2499	212 ± 24	129 ± 21	56 ± 20	341 ± 38	397 ± 53
Diabetic + 4% ethanol	2821 ± 348	10860 ± 1380	182 ± 15	180 ± 22	56 ± 11	362 ± 18	419 ± 22
ANOVA	$p \leq 0.053$	$p \leq 0.099$	$p \leq 0.111$	$p \leq 0.187$	$p \leq 0.432$	$p \leq 0.142$	$p \leq 0.164$
Experiment 2 (10 weeks)							
Control	3477 ± 758	13640 ± 3010	136 ± 20	106 ± 8	30 ± 4	242 ± 22	272 ± 23
Ethanol (4%)	2919 ± 284	11400 ± 1126	165 ± 9	96 ± 10	33 ± 3	261 ± 19	294 ± 21
Ethanol (12%)	3116 ± 704	12220 ± 2788	127 ± 13	94 ± 14	30 ± 5	221 ± 27	250 ± 30
Diabetic	3687 ± 562	13760 ± 1833	173 ± 11	193 ± 9†	64 ± 6‡	367 ± 61†	430 ± 83‡
Diabetic + ethanol (4%)	2740 ± 390	10370 ± 1972	161 ± 14	160 ± 12†	45 ± 6	309 ± 19§	350 ± 24§
ANOVA	$p \leq 0.816$	$p \leq 0.817$	$p \leq 0.071$	$p \leq 0.001$	$p \leq 0.001$	$p \leq 0.003$	$p \leq 0.001$

* $p \leq 0.05$ vs. D and DE4 (experiment 1); † $p \leq 0.05$ vs. C, E4, E12 (experiment 2); ‡ $p \leq 0.05$ vs. all other groups (experiment 2); § $p \leq 0.05$ vs. C and E12 (experiment 2).

Table 3. Normalized image texture energy

	H1/image	V1/image	D1/image	H1 + V1/ image	H1 + V1 + D1/image
Experiment 1 (5 weeks)					
Control	0.052 ± 0.006	0.039 ± 0.004	0.010 ± 0.001	0.091 ± 0.001	0.101 ± 0.010
Ethanol (12%)	0.057 ± 0.007	0.040 ± 0.007	0.010 ± 0.001	0.097 ± 0.011	0.108 ± 0.011
Diabetic	0.101 ± 0.002*	0.058 ± 0.008	0.027 ± 0.009	0.159 ± 0.023†	0.186 ± 0.030†
Diabetic + 4% Ethanol	0.067 ± 0.008	0.066 ± 0.011	0.020 ± 0.003	0.133 ± 0.015	0.153 ± 0.014
ANOVA	$p \leq 0.018$	$p \leq 0.084$	$p \leq 0.076$	$p \leq 0.028$	$p \leq 0.021$
Experiment 2 (10 weeks)					
Control	0.044 ± 0.007	0.037 ± 0.008	0.010 ± 0.002	0.081 ± 0.012	0.091 ± 0.014
Ethanol (4%)	0.059 ± 0.005	0.034 ± 0.005	0.012 ± 0.001	0.093 ± 0.007	0.104 ± 0.008
Ethanol (12%)	0.053 ± 0.013	0.036 ± 0.006	0.012 ± 0.002	0.088 ± 0.019	0.100 ± 0.021
Diabetic	0.054 ± 0.006	0.056 ± 0.007‡	0.018 ± 0.001§	0.106 ± 0.014	0.127 ± 0.012
Diabetic + Ethanol (4%)	0.061 ± 0.008	0.065 ± 0.012§	0.017 ± 0.003‖	0.126 ± 0.014	0.143 ± 0.021
ANOVA	$p \leq 0.635$	$p \leq 0.025$	$p \leq 0.048$	$p \leq 0.217$	$p \leq 0.177$

* $p \leq 0.05$ vs. all other groups (experiment 1); † $p \leq 0.05$ vs. C and E12 (experiment 1); ‡ $p \leq 0.05$ vs. E4 (experiment 2); § $p \leq 0.05$ vs. C, E4, E12 (experiment 2); ‖ $p \leq 0.05$ C (experiment 2).

1998) previously in diabetic rats and rats receiving ethanol. The textural changes recorded from the cardiomyopathic rats were detected only by calculating detail coefficient energy from 2-D wavelet decomposition. Conventional statistical methodology was unable to discriminate between groups. We also found that other equations (log energy, Shannon's entropy) for calculating textural energy (Coifman and Wickerhauser 1992) were unable to improve our ability to discriminate between groups.

Our findings are in general agreement with a previous study evaluating patients in the early postmyocardial infarction period. By using the 2-D Haar wavelet decomposition method with an image extension algorithm, the horizontal detail (vertical edge) coefficient energy was able to predict eventual recovery of viable myocardium from that of myocardial necrosis (Neskovic et al. 1998). Our study differed in that the horizontal detail coefficient energy was not quite as sensitive as other detail coefficients. Our ability to utilize other detail coefficients, however, including diagonal coefficients, which previously were thought to contain mostly noise, probably was significantly aided by using a digital signal that had no smoothing or logarithmic compression and, importantly, had not been converted to a video signal and digitized again for processing.

We also evaluated energy by normalizing energy to the energy content of the original image ROI (Table 3). This technique, which preserves grey-scale transform invariance, identified increased textural energy in the diabetic animals at 5 weeks. Values for texture at 5 weeks tended to be lower in ethanol-treated diabetic rats than in untreated diabetic rats. Normalization of data may enhance the ability to discriminate between experimental groups at an early stage in the disease process. Because speckle size is a function of US beam depth and transducer focusing properties and, thus, machine-dependent, we kept machine settings constant for the entire study. Even under these conditions, normalization of the data appeared to enhance the ability to identify group differences at an early time.

Limitations of the study

In this study, we used the signal generated after digital scan conversion, and not the radiofrequency (RF) signal. Although this signal is influenced by transducer and machine characteristics, the RF signal is also. A comparison study of both signals would need to be performed, to see if there would be any advantage to use of the RF signal for analysis and quantitation of image texture.

Although US speckle (texture) is altered by tissue pathology, it is also influenced by the transducer and machine used, and by machine settings. Although we kept all settings constant for the study, we do not know if these quantitative textural differences are reproducible using other transducers and US equipment made by other manufacturers.

Differences in ability to differentiate myocardium were noted between the H1, V1 and D1 detail coefficients. These differences may in part be explained by anisotropy of myocardial scattering (Mottley and Miller 1988), and variations in texture in relation to the tissue distance from the transducer (Skorton et al. 1983b). For this study, we do not expect that variations in tissue distance from the transducer were problematic, in that all studies were performed with identical depth and focus settings.

Because image resolution is a function of the frequency and depth settings of the transducer, human studies would not achieve the spatial resolution that was

achieved in this study of cardiomyopathic laboratory rats.

CONCLUSION

The 2-D Haar wavelet image decomposition method appears to be a mathematical tool that may help identify early echocardiographic myocardial image textural changes in diabetes mellitus, even before the onset of M-mode structural changes. In addition, using the same digital image data, we found that first-order statistical measures of texture were unable to identify early myocardial abnormalities. It appears that the wavelet decomposition method may be able to identify early diabetic cardiomyopathy. Hence, this technique could be applicable in the follow-up of patients with diabetes mellitus, as well as in a variety of other clinical settings where the recognition of the evolution of subtle forms of diffuse myocardial tissue change might help guide treatment.

REFERENCES

Aldroubi A. The wavelet transform: A surfing guide. In: Aldroubi A, Unser M, eds. New York: CRC Press, 1996:3–36.

Batista A, English M. A multiresolution wavelet method for characterization of ventricular late potentials. IEEE Computers Cardiol 1996;23:625–628.

Bertrand O, Bohorquez J, Pernier J. Time-frequency digital filtering based on an invertible wavelet transform: An application of evoked potentials. IEEE Trans Biomed Eng 1994;41(1):77–88.

Bhandari AK, Nanda NC. Myocardial texture characterization by two-dimensional echocardiography. Am J Cardiol 1983;51:817.

Chandrasekaran K, Aylward PE, Fleagle SR, et al. Feasibility of identifying amyloid and hypertrophic cardiomyopathy with the use of computerized quantitative texture analysis of clinical echocardiographic data. J Am Coll Cardiol 1989;13(4):832–840.

Chang T, Kuo CCJ. Texture analysis and classification with tree-structured wavelet transform. IEEE Trans Image Process 1993;2: 429–441.

Chui CK. Wavelets. A mathematical tool for signal analysis. Philadelphia: Society for Industrial and Applied Mathematics, 1997:178–180.

Coifman RR, Wickerhauser MV. Entropy-based algorithms for best basis selection. IEEE Trans Information Theory 1992;38(2):713–718.

Daubechies I. Ten lectures on wavelets. Philadelphia: Society for Industrial and Applied Mathematics, 1992.

Ferdeghini EM, Pinamonti B, Picano E, et al. Quantitative texture analysis in echocardiography: Application to the diagnosis of myocarditis. J Clin Ultrasound 1991;19:263–270.

Gamero LG, Risk M, Sobh JF, Ramirez AJ, Saul JP. Heart rate variability analysis using wavelet transform. IEEE Computers Cardiol 1996;23:177–180.

Giles TD, Ouyang J, Kerut EK, et al. Changes in protein kinase C in early cardiomyopathy and in gracilis muscle in the BB/Wor diabetic rat. Am J Physiol 1998;274:H295–H307.

Gonzales RC, Woods RE. Digital image processing. Reading, MA: Addison-Wesley Publishing Company, 1992:508.

Haskell WL, Masuyama T, Nellessen U, et al. Serial measurements of integrated ultrasonic backscatter in human cardiac allografts for the recognition of acute rejection. Circulation 1990;81(3): 829–839.

IEEE. Standard glossary of image processing and pattern recognition terminology. Piscataway, NJ: IEEE Press, 1990.

Kim ND, Main V, Wilson D, Rouse G, Up S. Ultrasound image texture analysis for characterizing intramuscular fat content of live beef cattle. Ultrasonic Imaging 1998;20:191–205.

Mallat S. A theory for multiresolution signal decomposition: The wavelet representation. IEEE Trans Pattern Anal Machine Intell 1989;11:674–693.

Mallat S. Multifrequency channel decomposition of images and wavelet models. IEEE Trans Acoustics Speech Signal Process 1989;37: 2091–2110.

Marini C, Picano E, Varga A, et al. Cyclic variation in myocardial gray level as a marker of viability in man: A videodensitometric study. Eur Heart J 1996;17:472–479.

Mecocci A, Gamba P, Marazzi A, Barni M. Texture segmentation in remote sensing images by means of packet wavelets and fuzzy clustering. Int Soc Optical Eng Synth Aperture Radar Passive Microwave Sensing 1995;2584:142–151.

Meste O, Rix H, Caminal P, Thakor NV. Ventricular late potentials characterization in time-frequency domain by means of a wavelet transform. IEEE Trans Biomed Eng 1994;41(7):625–634.

Miller JG, Perez JE, Sobel BE. Ultrasonic characterization of myocardium. Prog Cardiovasc Dis 1985;28(2):85–110.

Mojsilovic A, Popovic MV, Neskovic AN, Popovic AD. Wavelet image extension for analysis and classification of infarcted myocardial tissue. IEEE Trans Biomed Eng 1997;44(9):856–866.

Mottley JG, Miller JG. Anisotropy of the ultrasonic backscatter of myocardial tissue: I. Theory and measurements in vitro. J Acoust Soc Am 1988;83(2):755–761.

Neskovic AN, Mojsilovic A, Jovanovic T, et al. Myocardial tissue characterization after acute myocardial infarction with wavelet image decomposition: A novel approach for the detection of myocardial viability in the early post infarction period. Circulation 1998; 98:634–641.

Picano E, Faletra F, Marini C, et al. Increased echo density of transiently asynergic myocardium in humans: A novel echocardiographic sign of myocardial ischemia. J Am Coll Cardiol 1993; 21(1):199–207.

Pinamonti B, Picano E, Ferdeghini EM, et al. Quantitative texture analysis in two-dimensional echocardiography: Application to the diagnosis of myocardial amyloidosis. J Am Coll Cardiol 1989; 13(4):832–840.

Prasad L, Lyengar SS. Wavelet analysis with applications to image processing. Boca Raton, FL: CRC Press, 1997:235–239, 258–262.

Press WH, Teukolsky SA, Vetterling WT, Flannery BP. Numerical recipes in FORTRAN: The art of scientific computing, 2nd ed. New York: Cambridge University Press, 1992:596–597.

Sagar KB, Pelc LR, Rhyne TL, et al. Role of ultrasonic tissue characterization to distinguish reversible from irreversible myocardial injury. J Am Soc Echocardiog 1990;3(6):471–477.

Sagar KB, Rhyne TL, Pelc LR, Warltier DC, Wann LS. Intramyocardial variability in integrated backscatter: Effects of coronary occlusion and reperfusion. Circulation 1987;75:436–442.

Sahn DJ, DeMaria AN, Kisslo J, Weyman AE. Recommendations regarding quantitation in M-mode echocardiography: Results of a survey of echocardiographic measurements. Circulation 1978;58: 1072.

Skorton DJ, Collins SM, Nichols J, et al. Quantitative texture analysis in two-dimensional echocardiography: Application to the diagnosis of experimental myocardial contusion. Circulation 1983a;68(1): 217–223.

Skorton DJ, Collins SM, Woskoff SD, Bean JA, Melton HE. Range- and azimuth-dependent variability of image texture in two-dimensional echocardiograms. Circulation 1983b;68(4):834–840.

Smith SW, Wagner RF. Ultrasound speckle size and lesion signal to noise ratio: Verification of theory. Ultrasonic Imaging 1994;6: 174.

Stempfle H, Angermann CE, Kraml P, et al. Serial changes during acute cardiac allograft rejection: Quantitative ultrasound tissue analysis versus myocardial histologic findings. J Am Coll Cardiol 1993;22(1):310–317.

Teolis A. Computational signal processing with wavelets. Boston: Birkhauser, 1998:59–78.

Unser M. A practical guide to the implementation of the wavelet transform. In: Aldroubi A, Unser M, eds. New York: CRC Press, 1996:37–73.

Van de Wouwer G, Scheunders P, Van Dyck D. Statistical texture characterization from discrete wavelet representations. IEEE Trans Image Process 1999;8(4):592–598.

Wagner RF, Smith SF, Sandrick JM, Lopez H. Statistics of speckle in ultrasound B-scans. IEEE Trans Sonics Ultrason 1983;SU-30: 156.

Walker JS. A primer on wavelets and their scientific applications. Boca Raton, FL: Chapman and Hall/CRC, 1999.

Wickerhauser MV. Adopted wavelet analysis from theory to software. Wellesley, MA: AK Peters, 1994:361–377.

Wickline SA, Thomas JL III, Miller JG, Sobel BE, Perez JE. Sensitive detection of the effects of reperfusion on myocardium by ultrasonic tissue characterization with integrated backscatter. Circulation 1986;74:389–400.

Wild JJ, Crafford HD, Reid JM. Visualization of the excised human heart by means of reflected ultrasound or echography. Am Heart J 1957;54:903–906.